METRICA
METRology Institutional CAtalog

ISTITUTO NAZIONALE DI RICERCA METROLOGICA
Repository Istituzionale

Observing the effect of polarization mode dispersion on nonlinear interference generation in wide-band optical links

(Article begins on next page)

22 September 2024

Observing the effect of polarization mode dispersion on nonlinear interference generation in wide-band optical links

DARIO PILORI,[1,2,*] 🆔 MATTIA CANTONO,[1,3] 🆔 ALESSIO FERRARI,[1] 🆔 ANDREA CARENA,[1] 🆔 AND VITTORIO CURRI[1] 🆔

[1]*DET, Politecnico di Torino, Corso Duca degli Abruzzi 24, Torino (TO), 10129, Italy*
[2]*Currently with INRiM, Strada delle Cacce 91, Torino (TO), 10135, Italy*
[3]*Currently with Google LLC, 1600 Amphitheatre Parkway, Mountain View, CA 94043, USA*
[*]*d.pilori@inrim.it*

Abstract: With the extension of the spectral exploitation of optical fibers beyond the C-band, accurate modeling and simulation of nonlinear interference (NLI) generation is of the utmost performance. Models and numerical simulation tools rely on the widely used Manakov equation (ME): however, this approach when also considering the effect of polarization mode dispersion (PMD) is formally valid only over a narrow optical bandwidth. In order to analyze the range of validity of the ME and its applicability to future wide-band systems, we present numerical simulations, showing the interplay between NLI generation and PMD over long dispersion-uncompensated optical links, using coherent polarization division multiplexing (PDM) quadrature amplitude modulation (QAM) formats. Using a Monte-Carlo analysis of different PMD realizations based on the coupled nonlinear Schrödinger equations, we show that PMD has a negligible effect on NLI generation, independently from the total system bandwidth. Based on this, we give strong numerical evidence that the ME can be safely used to estimate NLI generation well beyond its bandwidth of validity that is limited to the PMD coherence bandwidth.

1. Introduction

To increase the capacity of coherent optical systems and re-configurable and transparent optical networks [1,2] with respect the present level a viable solution is to extend the exploited optical bandwidth beyond the currently used spectral region in the C-band [3]. In this transmission scenario, the optical physical layer plays a crucial role on overall performances, since it affects network design, management and orchestration [4,5]. For this reason, predicting propagation impairments is a key enabler for performance optimization both in the planning and in the operation phase of an optical network [6]. It was widely shown that, with state-of-the-art transceivers based on polarization division multiplexing (PDM) and multilevel modulation formats with coherent detection, the main capacity-limiting effects are amplified spontaneous emission (ASE) noise introduced by optical amplifiers and nonlinear interference (NLI) [7]. While ASE noise is an additive white Gaussian noise (AWGN) source, NLI, in general, is not an AWGN [8]. However, it was shown that, in all most common conditions, NLI can be accurately approximated as an AWGN source [9]. This key simplifying approximation allows the development of simple and effective models to predict the power spectral density of the generated NLI [10–12]. These models are then used to derive quality of transmission (QoT) estimators, which are crucial to assess physical layer impairments of optical networks [4].

All NLI models for coherent PDM optical transmission assume that fiber Kerr effect is governed by the Manakov equation (ME) [13,14], which is an approximation of the dual-polarization coupled nonlinear Schrödinger equation (DP-NLSE) with random birefringence. The ME averages out the birefringence, assuming that the local orientation of its axes do not significantly

vary with frequency. This allows the derivation of simple analytical expressions, which are exploited to derive NLI models. However, in the presence of polarization mode dispersion (PMD), this equation is formally valid only over a narrow optical bandwidth, called PMD coherence bandwidth [13,15–17]. Therefore, this undermines the validity of NLI models for wide-band systems. In [18] the authors performed extensive numerical simulations on the impact of PMD on coherent systems on dispersion-compensated (and uncompensated) systems, showing a small reduction of NLI in the presence of PMD. However, the conditions considered in that work (number of WDM channels, pulse shaping filter) are significantly different from modern ultra-wide-band scenarios, which may reduce the application of those results over such modern scenarios. On the other hand, recent experimental demonstrations of coherent transmission well beyond the PMD coherence bandwidth [19–22], have shown a substantial agreement between models and measurements. This suggests that the ME, at least for transmission of coherent signals over long dispersion-uncompensated links, can be valid also for wide optical bandwidths, and, consequently, we infer that PMD plays a negligible role in NLI generation.

PMD is a stochastic effect, and a thorough study of NLI generation in the presence of PMD requires Monte-Carlo analyses over a large set of realizations. Consequently, numerical simulations are the only suitable method to perform this particular kind of analysis. Moreover, with numerical simulations the PMD parameter δ_{PMD} can be tuned to overly large values, even if not realistic, in order to enhance any possible PMD-induced NLI modification.

In [23], we have presented a preliminary study of NLI generation in wide optical bandwidth systems considering the presence of PMD: our results confirmed the validity of the ME over such bandwidths. This article extends it, by providing additional results and further insights and it is organized as follows. First, in Sec. 2.1 the system scenario under analysis is described. Then, in Sec. 2.2, it is illustrated the numerical simulator based on the PMD *coarse-step* method [13] used to simulate PMD in a split-step Fourier method (SSFM) simulation. Results are presented in Sec. 3: we analyzed propagation of a system with up to 81 channels carrying a 32-GBaud PDM-QAM modulations with standard 50 GHz spacing, corresponding to a maximum optical bandwidth B_{WDM} of approximately 4 THz. We simulated the system relying either on the ME or on the coupled DP-NLSE including Monte-Carlo analyses of the PMD effect. Finally, conclusions are delineated in Sec. 4.

2. Simulation setup

2.1. System scenario

In this work we consider a wide-band coherent transmission of PDM-QAM signals, over long dispersion-uncompensated links. A schematic of the analyzed link is depicted in Fig. 1. N_{ch} transmitters generate PDM-QPSK or PDM-16-QAM signals at 32 GBaud, shaped with root-raised-cosine filters having 15% roll-off. The WDM channels, which are 50 GHz spaced around the central frequency $f_0 = 193.4$ THz, are propagated over 20×100-km spans of G.652 fiber (SMF) with typical parameters: loss of 0.2 dB/km, dispersion of -21.27 ps^2/km and effective area of 80 μm^2, giving a 1.3 1/(W km) nonlinear coefficient. After each fiber span, a flat-gain EDFA with noise figure $F = 5$ dB fully recovers span loss. Intra-channel stimulated Raman scattering (ISRS) is neglected, since the purpose of this work is only the analysis of the effect of PMD on Kerr-induced NLI generation.

At the receiver, we consider as channel-under-test (CUT) the central channel of the WDM comb, and we apply a polarization and phase diversity coherent receiver. After photodetection and analog-to-digital conversion, signals are equalized by an LMS adaptive equalizer with 17 taps, and the generalized signal-to-noise ratio (SNR) is evaluated on the constellation. As both channel and local oscillator lasers are assumed ideal, no carrier phase estimation (CPE) is performed. The parameters of the equalizer were carefully chosen to have a negligible (i.e. less than 0.01 dB) penalty, both in back-to-back and after fiber propagation.
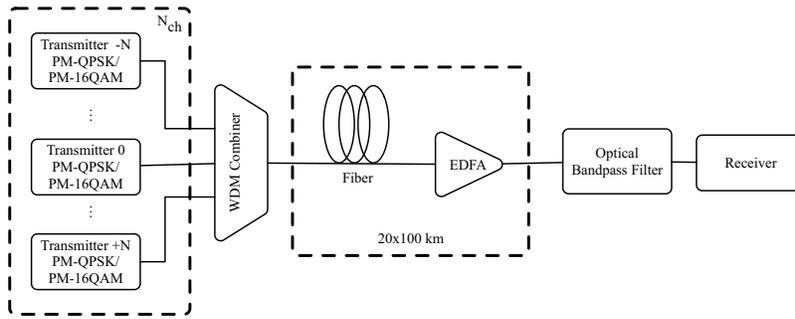
Fig. 1. General schematic of the simulation scenario.

2.2. *Numerical simulator*

Fiber propagation is emulated with a GPU-assisted implementation of the SSFM [24,25]. We analyzed the system using both the coupled DP-NLSE and the ME equations. When applied to the DP-NLSE, the SSFM is integrated with the coarse step method [13] to consider the random birefringence evolution that determines PMD. Such method approximates the continuous birefringence variations of a realistic fiber by a concatenation of fixed-length birefringent sections, each of them characterized by a random orientation of its principal states of polarization (PSP) axis and a given differential group delay (DGD). PSP are a special orthogonal pairs of polarization, characterized by the fact that light launched in a PSP does not change polarization at the output. [15]. To avoid resonance effects, we randomized the waveplate length as suggested in [13,26,27]. The coarse step method is integrated in the linear step of the SSFM as described in [24]. As a reference, we also propagated the investigated signals with the PMD effect averaged out, integrating the ME. When applying the DP-NLSE, we performed Monte-Carlo investigations of fiber propagation with PMD parameter first set at δ_{PMD} = 0.05 ps/$\sqrt{km}$ and then at 1 ps/$\sqrt{km}$. While the first value represents a typical value for modern G.652 fibers, the latter is an overly large value that we adopted to have a polarization coherence bandwidth, where the ME should be valid, as narrow as [15,28]:

$$\sqrt{\frac{3}{4\pi^2\delta_{PMD}^2 L_{eff}}} \approx 65 \text{ GHz}. \tag{1}$$

This value was chosen to trigger any possible interaction between PMD and NLI generation out of the ME validity bandwidth, *i.e.*, beyond the limits of NLI generation modeling.

3.   **Results and discussion**

We first measured the SNR on the reference scenario (20 × 100 km SMF) as a function of the per-channel launch power P_{ch}. Results are shown in Fig. 2 and Fig. 3 for PDM-QPSK (a) and PDM-16-QAM (b) respectively. One curve refer to the ME and two to the different values of δ_{PMD} analyzed using the DP-NLSE. For these first results, we measured only a single PMD realization.

In Fig. 2 results are shown for the case of with N_{ch} = 21 WDM channels, which correspond approximately to B_{WDM} = 1 THz. This value of bandwidth is larger than the PMD coherence bandwidth for δ_{PMD} = 1 ps/$\sqrt{km}$, whilst is smaller than PMD coherence bandwidth for 0.05 ps/$\sqrt{km}$ (which is ∼ 1.2 THz). While at low values of P_{ch}, where performance is ASE-noise limited, all the three cases give the same SNR, simulations with larger values of PMD give *slightly* lower performances with the increase of power. This suggests that PMD, in this case, slightly increases the amount of NLI generated. At P_{ch} = 0 dBm, which is the optimal power

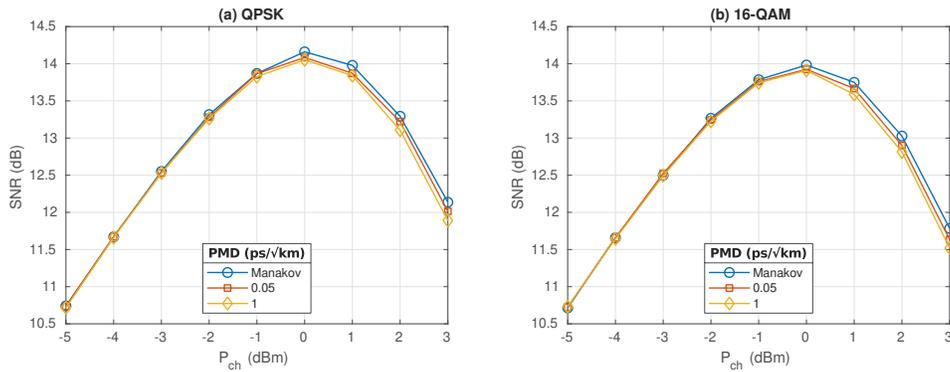**Fig. 2.** SNR as a function of the per-channel launch power P_{ch} with $N_{ch} = 21$ WDM channels ($B_{WDM} \approx 1$ THz).

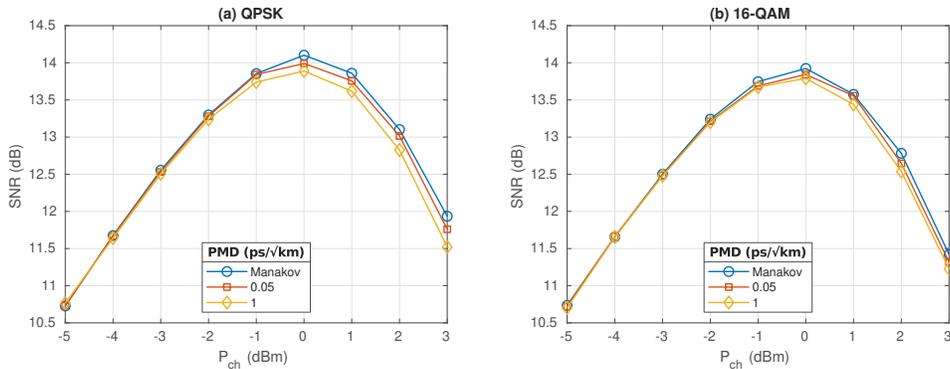**Fig. 3.** SNR as a function of the per-channel launch power P_{ch} with $N_{ch} = 41$ WDM channels ($B_{WDM} \approx 2$ THz).

value, the difference of SNR values obtained using ME and DP-NLSE is 0.11 dB for PDM-QPSK and 0.07 dB for PDM-16-QAM respectively, for the case of $\delta_{PMD} = 1$ ps/$\sqrt{km}$: there is a larger increase of NLI in lower-cardinality constellations.

Then, we repeated simulations doubling the number of channels ($N_{ch} = 41$, $B_{WDM} \approx 2$ THz): results are shown in Fig. 3. In this case, the optical bandwidth B_{WDM} is larger than the PMD coherence bandwidth for both values of δ_{PMD}. The trend is identical to the previous case when $N_{ch} = 21$. The only observed difference is a small increase in the SNR gap at $P_{ch} = 0$ dBm and $\delta_{PMD} = 1$ ps/$\sqrt{km}$, which is now 0.21 dB for PDM-QPSK and 0.13 dB for PDM-16-QAM. These results strongly suggest that PMD coherence bandwidth plays a negligible role in NLI generation.

In this latter case ($N_{ch} = 41$), we ran 20 simulations and we averaged out results. Since PMD is a stochastic effect, simulations must be verified with a Monte-Carlo analysis over different realizations: we repeated 20 times simulations of the $N_{ch} = 41$ case previously analyzed at $P_{ch} = 0$ dBm with different statistical realizations of random birefringence. Results are reported in Fig. 4: we show the cumulative average of the SNR at the highest PMD value $\delta_{PMD} = 1$ ps/$\sqrt{km}$. After few realizations, the cumulative average converges to a stable result with an extremely low standard deviation (<0.03 dB). Consequently, we conclude that the results of Fig. 3 do not depend on a specific PMD realization.
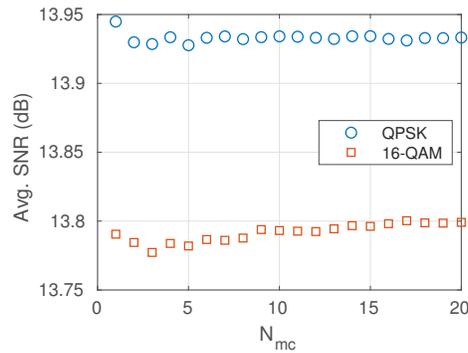
Fig. 4. Cumulative average of the SNR over 20 different PMD realizations (N_{mc}) at $P_{ch} = 0$ dBm with $N_{ch} = 41$ WDM channels ($B_{WDM} \approx 2$ THz) and $\delta_{PMD} = 1$ ps/$\sqrt{\text{km}}$.

3.1. Effect of PMD on signal statistics

To find a possible explanation of the *small* SNR difference, we run a numerical simulation over a PMD-only fiber, *i.e.* an optical fiber without attenuation, dispersion and Kerr effect ($\alpha = 0$, $\beta_2 = 0$, $\gamma = 0$). The simulation was run over 23 km of fiber, which corresponds approximately to the effective length of the span. We then measured the signal histograms before (Fig. 5a) and after (Fig. 5b) propagation over this optical fiber. Since a modulated signal is a cyclostationary random process [29], with periodicity equal to the symbol duration T, one needs to create several histograms of the signal at different time instants within a symbol. The obtained result is very similar to an eye diagram, as shown in Fig. 5. The Figure shows 24 different histograms of one quadrature of a 32-GBaud PDM-QPSK signal shaped with a 15% roll-off root-raised-cosine shaping filter. The number of symbols used in the simulation was 20 000. For this simulation, PMD has been further increased to very large value of 5 ps/$\sqrt{\text{km}}$ to exacerbate its effects on the signal and to allow a qualitative inspection of the histogram. Comparing Fig. 5(a) with (b), it can be seen a slight spread of the duration of the symbol (yellow area at $T = 0$). This effect is similar (albeit much smaller) to the "Gaussianization" effect of chromatic dispersion (c), which makes the signal similar to a Gaussian distribution. According to NLI generation models [11,12], a Gaussian-distributed constellation generates more NLI. Consequently, this suggests that PMD, by "spreading" the signal, slightly increases NLI generation, as shown in Fig. 2 and 3. We remark that this effect is different from the reduction of the efficiency of cross phase modulation (XPM) caused by chromatic dispersion [8], which reduces the generation of NLI.
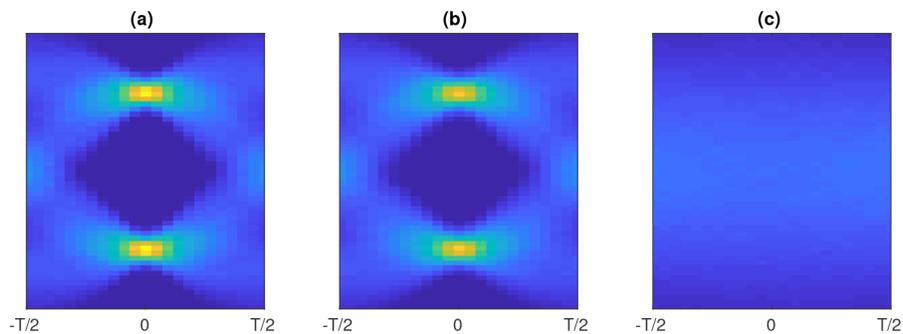

Fig. 5. Eye diagram of a 32-GBaud PDM-QPSK signal at the transmitter (a) and after 23 km of PMD-only fiber ($\alpha = 0$, $\beta_2 = 0$, $\gamma = 0$, $\delta_{PMD} = 5$ ps/$\sqrt{\text{km}}$) (b) and CD-only fiber (c). T is the symbol duration.

3.2. Propagation over low-dispersion fiber

In the previous results, we have shown evidence that, in the considered scenario, PMD slightly increases NLI generation. To give further evidence to this fact, we performed the same simulation over a different scenario. In particular, we simulated the same setup of Fig. 1, with $N_{ch} = 21$ WDM channels, over different fiber spans. The spans were made by standard G.655 Non-Zero Dispersion Shifted Fiber (NZDSF), with typical parameters: attenuation 0.222 dB/km, Kerr coefficient 1.4 1/(W km) and dispersion 3.8 ps/(nm km). Span length was reduced to 90-km in order to have the same span attenuation as 100-km SMF. Also the number of spans was reduced to 12, since we expect a stronger NLI generation, and consequently a shorter reach. The stronger difference between this scenario, and the SMF setup, is the amount of cumulated chromatic dispersion. In this case, chromatic dispersion is significantly lower than previous case, and it may give different results.

Results are shown in Fig. 6, and they are similar to SMF results (Fig. 2). In fact, also in this case PMD induces a small increase of NLI, which is stronger on PDM-QPSK. Consequently, we can conclude that the effect that is measured over SMF does not depend on that specific scenario, but it is also present on a different scenario, with a significantly smaller amount of cumulated chromatic dispersion.
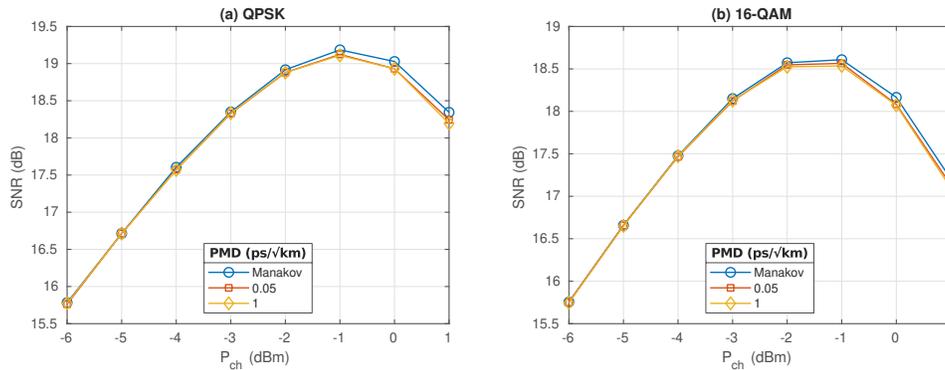

Fig. 6. SNR as a function of the per-channel launch power P_{ch} with $N_{ch} = 21$ WDM channels over 12×90 km of NZDSF.

3.3. Extending the optical bandwidth

To investigate the bandwidth dependence of this effect, we measured the SNR at fixed $P_{ch} = 0$ dBm by varying the number of WDM channels, i.e. the system optical bandwidth. Results are shown as markers in Fig. 7 with $N_{ch} = 11, 21, 31, 41, 61, 81$ WDM channels. While at low values of optical bandwidth the three results are closer, by increasing the optical bandwidth the gap slightly increases and then it keeps approximately constant. This suggests that this PMD-induced increase of NLI is not bandwidth-dependent. Moreover, results in Fig. 7 clearly indicate an increase of NLI proportional to $\log(B_{WDM})$, which is the increase predicted by NLI models [10–12] based on the ME. This can be seen by comparing in Fig. 7 the experimental results (markers) with the black dashed line, which is a best-fit of a linear decrease of SNR as a function of the logarithm of the optical bandwidth. Therefore, these results suggest that, in the considered scenario, the Manakov equation is valid up to optical bandwidths much larger than PMD coherence bandwidth. Moreover, these results are consistent with the experimental demonstrations presented in [19–21].
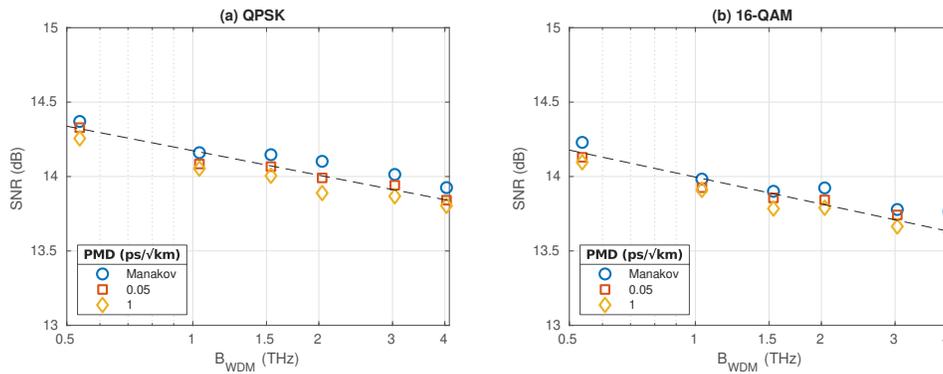
Fig. 7. SNR as a function of the total optical bandwidth B_{WDM} with fixed per-channel launch power $P_{\text{ch}} = 0$ dBm. Dashed line is a best-fit of an SNR decrease proportional to the logarithm of the optical bandwidth.

4. Conclusion

In this paper, we presented an extensive number of simulations of wide-band transmission of PDM-QAM signals over a long, dispersion-uncompensated link. We compared results obtained with the ME and with the DP-NLSE with two different values of PMD. We found that, in this scenario, the PMD coherence bandwidth plays a negligible role in NLI generation. Moreover, we also found that PMD *slightly* increase the power of NLI. This can be due to a change of signal statistics that enhances NLI generation. Measuring NLI generation as a function of the optical bandwidth, we observed a logarithmic increase of NLI with bandwidth, as predicted by models based on the ME. These results agree with recent experimental demonstrations, and strongly suggest that PMD plays a negligible role in NLI generation over such systems. However, a rigorous answer requires a thorough theoretical investigation, which is left for future research.

Acknowledgement

References

1. G. Rizzelli, G. Maier, M. Quagliotti, M. Schiano, and A. Pattavina, "Assessing the scalability of next-generation wavelength switched optical networks," J. Lightwave Technol. **32**(12), 2263–2270 (2014).
2. P. J. Winzer, D. T. Neilson, and A. R. Chraplyvy, "Fiber-optic transmission and networking: the previous 20 and the next 20 years [invited]," Opt. Express **26**(18), 24190 (2018).
3. M. Ionescu, D. Lavery, A. Edwards, E. Sillekens, L. Galdino, D. Semrau, R. Killey, W. Pelouch, S. Barnes, and P. Bayvel, "74.38 tb/s transmission over 6300 km single mode fiber with hybrid edfa/raman amplifiers," in *Optical Fiber Communication Conference (OFC) 2019*, (Optical Society of America, 2019), p. Tu3F.3.
4. V. Curri, M. Cantono, and R. Gaudino, "Elastic all-optical networks: A new paradigm enabled by the physical layer. how to optimize network performances?" J. Lightwave Technol. **35**(6), 1211–1221 (2017).
5. J.-L. Augé, G. Grammel, E. le Rouzic, V. Curri, G. Galimberti, and J. Powell, "Open optical network planning demonstration," in *Optical Fiber Communication Conference (OFC) 2019*, (Optical Society of America, 2019), p. M3Z.9.
6. M. Filer, M. Cantono, A. Ferrari, G. Grammel, G. Galimberti, and V. Curri, "Multi-vendor experimental validation of an open source qot estimator for optical networks," J. Lightwave Technol. **36**(15), 3073–3082 (2018).
7. M. Secondini and E. Forestieri, "Scope and limitations of the nonlinear Shannon limit," J. Lightwave Technol. **35**(4), 893–902 (2017).
8. R. Dar, M. Feder, A. Mecozzi, and M. Shtaif, "Properties of nonlinear noise in long, dispersion-uncompensated fiber links," Opt. Express **21**(22), 25685 (2013).
9. P. Poggiolini and Y. Jiang, "Recent advances in the modeling of the impact of nonlinear fiber propagation effects on uncompensated coherent transmission systems," J. Lightwave Technol. **35**(3), 458–480 (2017).

10. P. Poggiolini, G. Bosco, A. Carena, V. Curri, Y. Jiang, and F. Forghieri, "The GN-model of fiber non-linear propagation and its applications," J. Lightwave Technol. **32**(4), 694–721 (2014).

11. A. Carena, G. Bosco, V. Curri, Y. Jiang, P. Poggiolini, and F. Forghieri, "EGN model of non-linear fiber propagation," Opt. Express **22**(13), 16335–16362 (2014).

12. R. Dar, M. Feder, A. Mecozzi, and M. Shtaif, "Accumulation of nonlinear interference noise in fiber-optic systems," Opt. Express **22**(12), 14199 (2014).

13. D. Marcuse, C. R. Manyuk, and P. K. A. Wai, "Application of the Manakov-PMD equation to studies of signal propagation in optical fibers with randomly varying birefringence," J. Lightwave Technol. **15**(9), 1735–1746 (1997).

14. G. Agrawal, *Nonlinear Fiber Optics* (Elsevier Science Publishing Co Inc, 2012).

15. A. Galtarossa and C. R. Menyuk, *Polarization mode dispersion* (Springer Science & Business Media, 2006).

16. A. Carena, V. Curri, R. Gaudino, P. Poggiolini, and S. Benedetto, "On the joint effects of fiber parametric gain and birefringence and their influence on ASE noise," J. Lightwave Technol. **16**(7), 1149–1157 (1998).

17. C. J. McKinstrie, H. Kogelnik, R. M. Jopson, S. Radic, and A. V. Kanaev, "Four-wave mixing in fibers with random birefringence," Opt. Express **12**(10), 2033 (2004).

18. P. Serena, N. Rossi, O. Bertran-Pardo, J. Renaudier, A. Vannucci, and A. Bononi, "Intra- versus inter-channel PMD in linearly compensated coherent PDM-PSK nonlinear transmissions," J. Lightwave Technol. **29**(11), 1691–1700 (2011).

19. R. Pastorelli, G. Bosco, A. Carena, P. Poggiolini, V. Curri, S. Piciaccia, and F. Forghieri, "Investigation of the dependence of non-linear interference on the number of WDM channels in coherent optical networks," in *Proc. 38th European Conf. and Exhibition Optical Communications*, (2012), pp. 1–3.

20. G. Saavedra, M. Tan, D. J. Elson, L. Galdino, D. Semrau, M. A. Iqbal, I. D. Phillips, P. Harper, A. Ellis, B. C. Thomsen, D. Lavery, R. I. Killey, and P. Bayvel, "Experimental analysis of nonlinear impairments in fibre optic transmission systems up to 7.3 THz," J. Lightwave Technol. **35**(21), 4809–4816 (2017).

21. D. J. Elson, G. Saavedra, K. Shi, D. Semrau, L. Galdino, R. Killey, B. C. Thomsen, and P. Bayvel, "Investigation of bandwidth loading in optical fibre transmission using amplified spontaneous emission noise," Opt. Express **25**(16), 19529–19537 (2017).

22. M. Cantono, A. Ferrari, D. Pilori, E. Virgillito, J. L. Augé, and V. Curri, "Physical layer performance of multi-band optical line systems using Raman amplification," J. Opt. Commun. Netw. **11**(1), A103 (2019).

23. M. Cantono, D. Pilori, A. Ferrari, A. Carena, and V. Curri, "Observing the interaction of PMD with generation of NLI in uncompensated amplified optical links," in *Optical Fiber Communications Conference (OFC)*, (OSA, 2018).

24. D. Pilori, M. Cantono, A. Carena, and V. Curri, "FFSS: The fast fiber simulator software," in *Transparent Optical Networks (ICTON), 2017 19th International Conference on*, (IEEE, 2017), pp. 1–4.

25. S. Musetti, P. Serena, and A. Bononi, "On the accuracy of split-step fourier simulations for wideband nonlinear optical communications," J. Lightwave Technol. **36**(23), 5669–5677 (2018).

26. P. K. A. Wai and C. R. Menyak, "Polarization mode dispersion, decorrelation, and diffusion in optical fibers with randomly varying birefringence," J. Lightwave Technol. **14**(2), 148–157 (1996).

27. M. Eberhard and C. Braimiotis, "Numerical implementation of the coarse-step method with a varying differential-group delay," in *Optical Networks and Technologies*, (Kluwer Academic Publishers, 2005), pp. 530–534

28. M. Shtaif, A. Mecozzi, and J. A. Nagel, "Mean-square magnitude of all orders of polarization mode dispersion and the relation with the bandwidth of the principal states," IEEE Photonics Technol. Lett. **12**(1), 53–55 (2000).

29. W. A. Gardner, A. Napolitano, and L. Paura, "Cyclostationarity: Half a century of research," Signal Processing **86**(4), 639–697 (2006).

30. M. Cantono, "Physical layer aware optical networks," Ph.D. thesis, Politecnico di Torino (2018).